Journal of Sustainability Science and Management
Volume 18 Number 10, October 2023: 126-137
eISSN: 2672-7226

ELECTROCHEMICAL PERFORMANCE OF ZINC OXIDE NANOPARTICLES PREPARED VIA GREEN SYNTHESIS ROUTE USING CHROMOLAENA ODORATA LEAVES EXTRACT AS POTENTIAL ANODE MATERIAL IN SODIUM-ION BATTERY

NURUL ATIKAH IDRIS[1], NUR ATHIFAH ABDUL AZIZ [1], HANIS MOHD YUSOFF[1,2]*, NURUL HAYATI IDRIS[3], NURHANNA BADAR[1,2], KELIMAH ELONG[4], FARHANINI YUSOFF[1], CHIA POH WAI[1] AND NORHAFIEFA HASSAN[5]

[1]Faculty of Science and Marine Environment, Universiti Malaysia Terengganu, 21030 Kuala Nerus, Terengganu, Malaysia. [2]Advance Nano Materials (ANoMa) Research Group, Faculty of Science and Marine Environment, Universiti Malaysia Terengganu, 21030 Kuala Nerus, Terengganu, Malaysia. [3]Faculty of Ocean Engineering Technology and Informatic, Universiti Malaysia Terengganu, 21030 Kuala Nerus, Terengganu, Malaysia. [4]Centre for Functional Materials and Nanotechnology, Institute of Science, Universiti Teknologi MARA, 40450 Shah Alam, Malaysia. [5]Smart Paint Manufacturing Sdn Bhd No. 9 and 11, Jalan Indah Gemilang, 81800 Ulu Tiram, Johor, Malaysia.

**Corresponding author: hanismy@umt.edu.my*
Submitted final draft: 16 July 2023 *Accepted: 30 July 2023* http://doi.org/10.46754/jssm.2023.10.008

Abstract: A paradigm shift in the preparation of nanoparticles from a chemical synthetic route to the green synthetic method using plant extractives has gained much impetus. This study used Chromolaena odorata leaf extract to prepare zinc oxide nanoparticles (ZnO-NPs). The ZnO-NPs were characterised by spectroscopic, optical and thermal techniques. Thermogravimetric Analysis (TGA) revealed no significant weight loss observed after 550°C for precursor powder which was further calcined using a furnace at 800°C and 900°C to obtain ZnO-NPs. Fourier Transform Infrared Spectroscopy (FTIR) spectroscopy analysis indicated Zn-O stretching between 400 cm^{-1} to 500 cm^{-1}. UV-Vis spectra show a strong absorption band at 388 nm for both calcination temperatures. Scanning Electron Microscopy (SEM) images showed the irregular shapes of the samples at different calcinations. The X-ray diffraction (XRD) diffractograms showed that the synthesised ZnO-NPs are in a hexagonal wurtzite structure. Studies of the electrochemical performance showed that ZnO-NPs made with *Chromolaena odorata* extract and calcined at 800°C have better cyclability than ZnO-NPs calcined at 900°C. Due to better cyclability, these ZnO-NPs can be applied as anode material in sodium-ion batteries.

Keywords: Nanoparticles, *Chromolaena odorata*, green synthesis, sodium-ion battery.

Introduction

Nanotechnology has given the field of science a new revolution. Nanotechnology aims to provide useful design, characterisation, production, and application of structures. The fabrication of devices and systems by controlling their nano-scale size and shapes (Vallinayagam *et al*., 2021). Furthermore, materials like nanostructures, nanoparticles (NPs), and nanocomposites are an outcome of nanotechnology (Yusoff *et al*., 2015; Nasrollahzadeh *et al*., 2019; Bandeira *et al*., 2020; Saidi *et al*., 2020; Ganasan *et al*., 2023). In this structural evolution in nanoscale material synthesis metal and metal oxide nanoparticles are widely studied and imparted to their wide range of applications (Yusoff *et al.,* 2015; 2020; 2021; Bandeira *et al.,* 2020; Saidi *et al.,* 2020; Yusoff *et al.,* 2021; Ramesh & Venkateswarlu, 2022).

Zinc oxide nanoparticles (ZnO-NPs) are known for their impressive properties such as antibacterial, antifungal, UV filtering properties, and high catalytic and photochemical activity along with these, it also exhibit great binding energy, broadband gap, high piezoelectric properties (Raut *et al*., 2013; Yedurkar *et al*., 2018). ZnO-NPs is an example of attractive metal oxide NP material with a high bond strength which contains optoelectronic short-

wavelength applications due to its large band gap (3.37 eV) and high exciton binding energy (60 meV) at room temperature (Vaseem *et al*., 2010).

Recently, the synthesis of ZnO-NPs is preferable towards biosynthesis, a technique of synthesising NPs using microorganisms and plants. This green, environmentally friendly, savvy, biocompatible methodology (Agarwal *et al*., 2017). Green synthesis of NPs is famous among researchers because of their non-hazardous and very eco-friendly nature (Yusoff *et al*., 2015; Bandeira *et al*., 2020; Thiyagarajulu *et al*., 2021; Sharma *et al*., 2021; Rodrigues *et al*., 2021; Dharmalingam *et al*., 2022). This method is also preferable due to its stability and high synthesis rate compared to the chemical method (Ramanarayanan *et al*., 2018; Bandeira *et al*., 2020; Yusoff *et al*., 2020).

Precipitation, hydrolysis, pyrolysis, sol-gel, hydrothermal, and solvothermal procedures for preparing ZnO-NPs employ toxic reagents, are time-consuming, and produce waste (Nava *et al.,* 2017; Gilavand *et al*., 2021; Droepenu *et al.,* 2021).

Because of the cost-effective, economic viability, non-toxic and eco-friendly green synthesis of metal or metal oxide NPs has generated researchers' interest in producing ZnO-NPs with various shapes and sizes (Vaseem *et al*., 2010; Yusoff *et al*., 2021). From a previous study, *Chromolaena odorata* leaves consist of bioactive compounds, where the polyphenolic flavonoid molecule demonstrates effectiveness as both reducing and capping agents used in the synthesis of metal oxide nanoparticles, which develop the potential for application in green synthesis processes (Buniyamin *et al*., 2022). This study focuses on the green synthesis of ZnO-NPs using *Chromolaena odorata* leaves extract and establishing their morphology and size. The obtained ZnO-NPs were investigated for their potential as anode material for sodium-ion batteries (SIBs). SIBs are an alternative to replace Lithium-ion Batteries (LIBs) since they share similar electrochemical natures. Only limited works have been reported for potential anode material for sodium-ion batteries (Wang *et al*., 2016; Qin *et al*., 2016; Durai *et al*., 2017; Wang *et al*., 2019).

Materials and Methods

Preparation of Chromolaena adorata Extract

Zinc acetate dehydrate (Sigma Aldrich) was used to prepare the zinc acetate dehydrate solution without further purification. 4 g of zinc acetate dehydrate was weighed and dissolved in 20 mL of distilled water. The solution was stirred for about 10 min (Yusoff *et al*., 2020).

Green Synthesis of ZnO-NPs

The preparations for ZnO-NPs were carried out according to the method published by Yusoff *et al*. (2020) with some modifications. 80 mL aqueous extract of *Chromolaena odorata* was mixed homogenously with 20 mL zinc acetate dehydrate solution at a fixed temperature of 75°C. A brown precursor precipitate was formed after continuous stirring for up to 10 hours (Figure 1). The precursor was kept in the oven at 80°C overnight to dry. The precursor was calcined at 800°C and 900°C for 6 hours in the furnace and white precipitate was obtained by grinding to get fine particles.

Figure 1: Formation of dark brown precipitate

Characterisation of ZnO-NPs

ZnO-NPs have been characterised by Thermogravimetric Analysis (TGA) from Perkin Elmer was used to determine the

amount of material weight change, either as a function of rising temperature or as a function of time, in an atmosphere of nitrogen, helium, air, other gas, or as a vacuum of up to 30 m Torr. Fourier Transform Infrared Spectroscopy (FTIR) spectrometer from Shimadzu was used to determine prominent characteristics of metal oxide. The optical properties of ZnO-NPs have been characterised by UV-Vis from Shimadzu. The ZnO-NPs were dispersed in distilled water and then the solutions were stirred for 10 min before UV-Vis measurement. Scanning Electron Microscopy (SEM) from JEOL was used to image the form, size and microstructure of the products, while X-ray diffractogram (XRD) from Rigaku was used to determine the structure of the ZnO-NPs.

Fabrication of Super Capacitor Electrode

The copper foil was cut into strips to prepare the supercapacitor electrode (1 cm x 2 cm). The copper foil was rinsed in ethanol for 15-30 min and the copper foil was dried with tissue paper. Each of the copper foil strips was weighed and recorded. One side of the foil has been labelled accordingly. ZnO-NPs have been acting as active material. For electrode paste, ZnO-NPs, carbon black, and polyvinylidene difluoride (PVDF) were weighed at 0.0150 g, 0.0004 g and 0.0001 g, respectively. The mixture was ground with mortar and pestle for 15 min. After that, a drop-by-drop of 1-methyl-2-pyrrolidine (NMP) was added. The homogenous slurry was pasted on a few pieces of labelled copper foil and dried at 100°C for 6 hours in the vacuum. After being dried for 6 hours, the copper foil with carbon paste was weighed. The weight range of active material was measured around 0.5 to 1.0 mg.

Electrochemical Performance

The electrochemical output testing was performed in a glove box packed with argon. The sodium foil was applied to the form of a coin (CR2032) that serves as the counter-electrode of reference. The electrolyte 1 M $NaClO_4$, was dissolved in propylene carbonate (PC) with 5% wt mixture. Fluoroethylene carbonate (FEC) and Whatman (GF/D) glass fibre are separators. On the battery test device (Neware Battery Analyser) at 0.013V, the galvanostatic charge/discharge tests were carried out. All the electrochemical tests were evaluated under room temperature and pressure.

Results and Discussion

Thermogravimetric Analysis (TGA)

TGA measured substance weight change as a function of temperature or isothermal time. The derivative weight loss curve can show the weight loss peak. The analysis was performed by gradually increasing the temperature and plotting the graph weight against the temperature.

Before calcination, four sets of precursor samples were analysed using TGA with a 1°C/min heating rate using argon gas. Figure 2 shows the TGA graph of all four samples. To test the consistency of the *Chromolaena odorata* extract-based ZnO-NP synthesis process, these four samples were synthesised individually. All four sets of TGA curves showed continuous weight loss of up to 650°C; after that, no significant weight loss was observed. From this result, the calcination temperature was chosen at 800°C and 900°C.

The slight weight loss, seen at about 200°C, is the elimination of moisture. Larger weight loss can be seen at 300°C, possibly caused by the degradation of chemicals in plant extract (Bandeira *et al*., 2020).

Fourier Transform-Infrared Spectroscopy (FTIR)

ZnO-NPs bond vibrations were measured using FTIR. The spectra were measured at a range from 4000 cm^{-1} to 400 cm^{-1} by using the KBr pellet method with a ratio for KBr and sample is 7:1. Figure 3 shows the comparative spectra of commercial ZnO, ZnO before calcined and calcined samples at 800°C and 900°C.

The FTIR spectra confirmed the presence of specific bands for several functional groups and the wide peak of all spectra shown between 3000

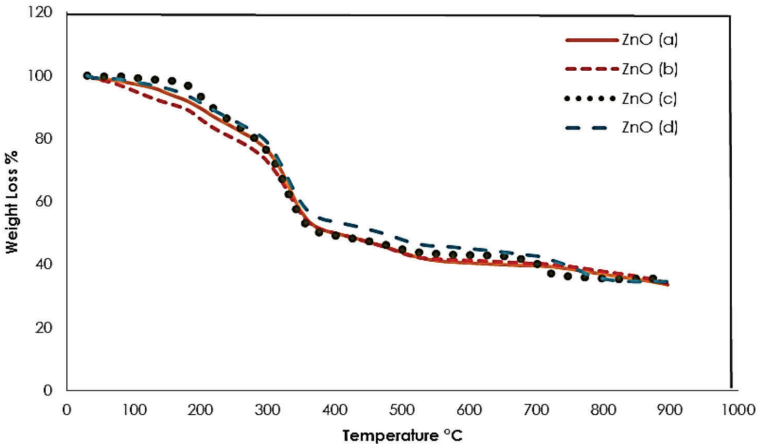

Figure 2: TGA graphs of four sets of precursor samples before calcination

and 3500 cm^{-1}. This has shown the occurrence of stretching vibrations of the O-H groups in water, and wide O-H peaks have narrowed with increased temperature calcination (Kayani *et al*., 2015; Fakhari *et al*., 2019; Yusoff *et al*., 2020).

The two peaks around 1650 to 1400 cm^{-1} correspond to either C-H bending or C-N stretching due to the presence of alkyl in *Chromolaena odorata* plants. C-O stretching causes a band between 1000 and 1100 cm^{-1} (Kayani *et al*., 2015; Dhanemozhi *et al*., 2017; Fakhari *et al*., 2019). The characteristic peak of the Zn-O stretching vibration peak appears at band 450 to 510 cm^{-1} in the spectra (Kayani *et al*., 2015; Dhanemozhi *et al*., 2017; Fakhari *et al*., 2019; Yusoff *et al*., 2020). Protein amino acids and amide associations stabilise ZnO-NPs, while phenolic compounds are related to the reduction process (Kayani *et al*., 2015; Dhanemozhi *et al*., 2017; Fakhari *et al*., 2019; Yusoff *et al*., 2020).

It can be argued that NPs are protected by compounds in the extract that can help prevent cluster formation (Datta *et al*., 2017). Table 1 summarises the band assignments of commercial ZnO, ZnO before calcined, and ZnO at 800°C. and 900°C.

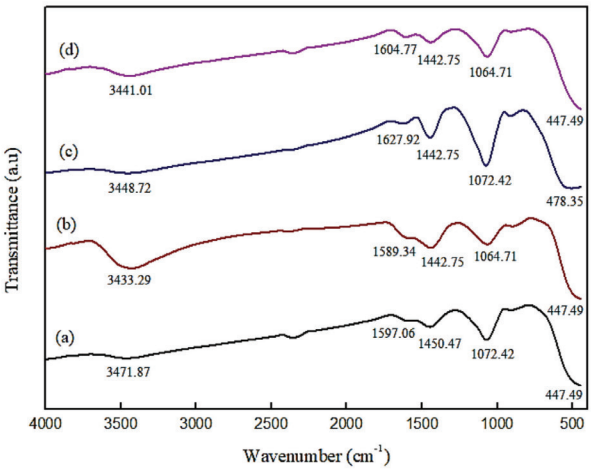

Figure 3: FTIR spectra of ZnO (a) commercial ZnO, (b) ZnO before calcined, (c) ZnO-NPs calcined at 800°C, and (d) ZnO-NPs calcined at 900°C

Table 1: Band assignments of commercial ZnO precursor before calcine, ZnO-NPs calcined at 800°C and 900°C

Band assignment	Characteristics Wavenumber (cm^{-1})			
	Commercial ZnO	ZnO before Calcine	ZnO-NPs Calcined at 800°C	ZnO-NPs Calcined at 900°C
O-H stretching	3471.87	3433.29	3448.72	3448.72
C-N stretching	1597.06/ 1450.47	1589.34/ 1442.75	1627.92/ 1442.75	1604.77/ 1442.75
C-O	1072.42	1064.71	1072.42	1064.71
Zn-O	447.49	447.49	478.35	447.49

UV-Visible Spectroscopy (UV-Vis)

Electromagnetic radiation, such as visible light, is mostly used as a wave phenomenon with wavelength or frequency characteristics (Dhanemozhi *et al*., 2017). UV-Vis of ZnO-NPs from previous studies has shown a sharp absorption peak range from 355 nm to 370 nm. Additionally, UV-Vis spectra are used to measure nanoparticles in size and shape (Darvishi *et al*., 2019). The UV-Vis absorption spectra from previous studies were recorded between 365 nm to 390 nm (Darvishi *et al*., 2019; Yusoff *et al*., 2020). Figure 4 shows UV-Vis spectra of ZnO-NPs calcined at 800°C and 900°C.

ZnO-NPs calcined at 800°C and 900°C show a prominent absorption band at 388 nm. This confirms that the synthesised products are ZnO only because the spectra showed no other peaks. These data confirm the presence of ZnO-NPs as the band of absorption obtained is quite similar to the previous research, showing a better result of ZnO-NPs absorption of UV. According to Chieng and Loo (2012), the ZnO-NPs that have absorption in the UV-Vis spectrum at a higher wavelength corresponded to the results of increasing particle size (Chieng *et al*., 2012). The band gap will increase due to an increment in particle size and calcination temperature.

Scanning Electron Microscopy (SEM)

SEM image shows the morphological, size details and surface of the ZnO commercial and ZnO synthesised by *Chromolaena odorata* extract under different calcination temperatures of 800°C and 900°C. Morphology samples are viewed under 3500X magnification with an

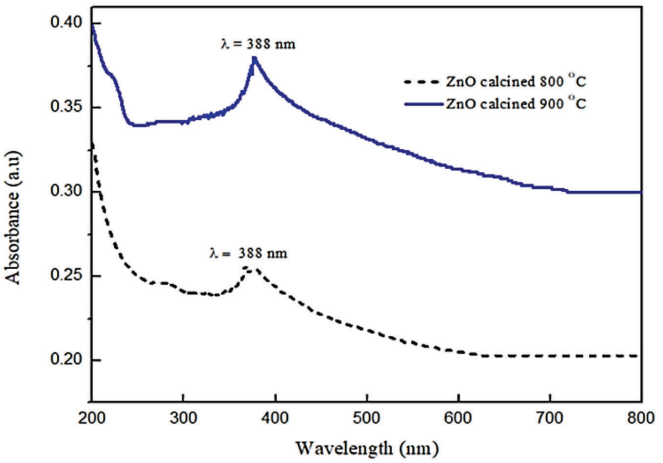

Figure 4: UV-Vis spectra of ZnO-NPs calcined at 800°C and 900°C

acceleration rate of 15 kV. Figure 5 shows the images obtained for commercial ZnO, ZnO-NPs calcined at 800°C and 900°C.

From the observations, the shapes of commercial ZnO ZnO-NPs calcined at 800ºC and 900°C are mixtures of irregular shapes. SEM determination showed the formation of ZnO-NPs as well as the dispersed and aggregation of the particles can be seen. ZnO-NPs synthesised using *Chromolaena odorata* appeared larger than commercial ZnO after calcination.

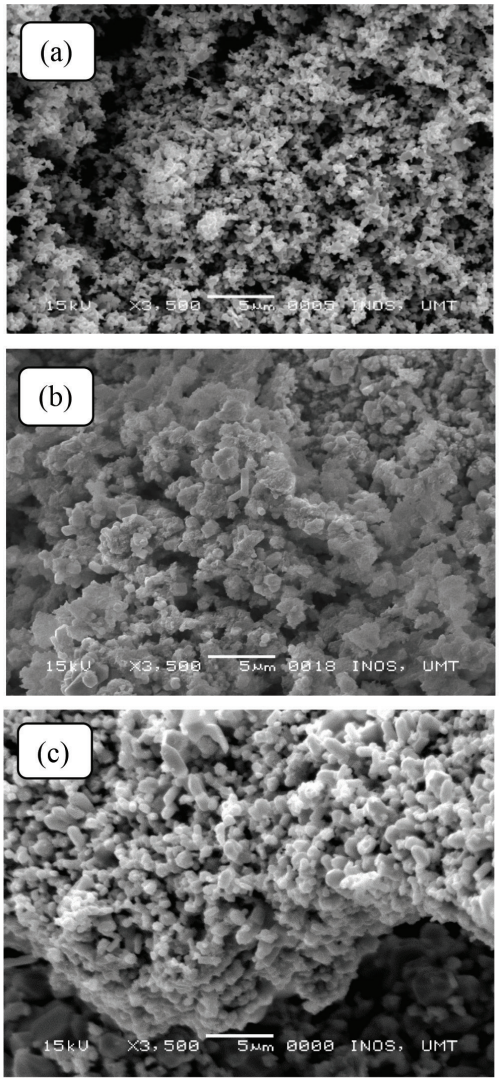

Figure 5: SEM images at 3500X magnification of (a) commercial ZnO, (b) ZnO-NPs calcined at 800°C, and (c) ZnO-NPs calcined at 900°C

This explains that it is possible to obtain ZnO-NPs with the same type of crystal but different particles due to the temperature of the calcination (Thirumavalavan *et al*., 2013; Yusoff *et al*., 2020). According to Dhanemozhi *et al*. (2017), improved surface morphology can be detected by increasing the temperature of calcination and obtaining larger particle sizes with small NP surface area (Ashraf *et al*., 2015; Dhanemozhi *et al*., 2017). Table 2 shows the size range of SEM micrographs for ZnO-NPs in several areas.

Table 2: Size range of SEM micrographs for ZnO-NPs synthesised using *Chromolaena odorata*

Sample	Size Range (nm)
Commercial ZnO	200–1000
ZnO-NPs calcined 800°C	700–1500
ZnO-NPs calcined 900°C	500–1500

X-ray Diffraction (XRD)

Figure 6 shows the XRD patterns of commercial ZnO and ZnO calcined at temperatures 800°C and 900°C. The crystallite sizes of commercial ZnO calcined at 800°C and 900°C calculated using the Scherrer formula, are shown in Table 3. The average crystallite size of commercial ZnO is 54 nm, while ZnO calcined at 800°C and 900°C are 27 nm and 28 nm, respectively.

Table 3 shows the data of XRD and d references (PDF 89-1397 and JCPDS 06-0644) of commercial ZnO, ZnO-NPs calcined at 800°C and 900°C. All the diffraction peaks are in the range of 20° to 80° it can be concluded that the structure of ZnO-NPs is in hexagonal wurtzite structure.

With an increase in calcination temperature, the intensity of diffraction peaks increases, indicating the strengthening of the ZnO phase (Ashraf *et al*., 2015). The three intense peaks correspond to the (100), (002), and (101) planes. The preferred orientation is observed along the (101) plane is observed.

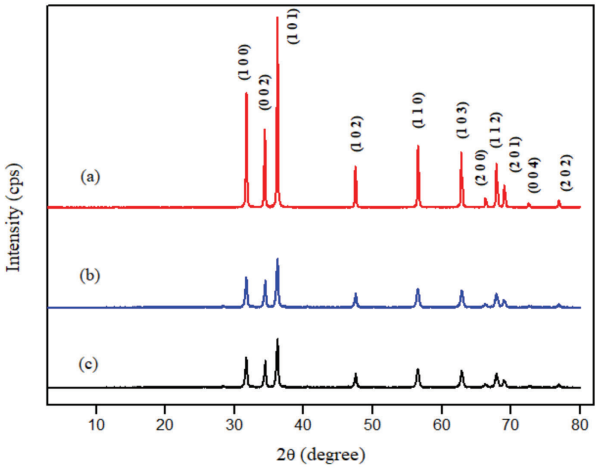

Figure 6: XRD diffractograms (a) commercial ZnO, (b) ZnO calcined at 800°C, and (c) ZnO calcined at 900°C

Table 3: Peak assignments of commercial ZnO and ZnO-NPs calcined at 800°C and 900°C for ZnO-NPs (Kayani *et al*., 2015; Ashraf *et al*., 2015; Yusoff *et al*., 2020). No peaks corresponding to the impurities were detected, so there are no peaks other than ZnO peaks and this verified that the pure ZnO-NPs were synthesised. The JCPDS 06-0644 data confirm these peaks and the wurtzite structure.

Samples	2θ	d (exp)	d (ref)	hkl	Crystallite Size (nm)	Peak Assignment
Commercial ZnO	31.72	2.819	2.817	100	44.35	ZnO
	34.35	2.608	2.606	002	42.94	ZnO
	36.19	2.480	2.478	101	42.92	ZnO
	47.47	1.914	1.913	102	39.30	ZnO
	56.52	1.627	1.626	110	37.40	ZnO
	62.79	1.479	1.479	103	64.11	ZnO
	66.30	1.409	1.408	200	58.28	ZnO
	67.88	1.380	1.379	112	60.61	ZnO
	69.01	1.360	1.359	201	57.93	ZnO
	72.52	1.302	1.303	004	82.55	ZnO
	76.90	1.239	1.239	202	64.26	ZnO
ZnO-NPs 800°C	31.74	2.817	2.814	100	29.05	ZnO
	34.48	2.599	2.604	002	32.51	ZnO
	36.23	2.478	2.478	101	27.55	ZnO
	47.53	1.911	1.912	102	30.74	ZnO
	56.51	1.627	1.627	110	23.56	ZnO
	62.84	1.478	1.478	103	22.96	ZnO
	66.28	1.409	1.409	200	24.27	ZnO
	67.88	1.380	1.380	112	23.18	ZnO
	68.98	1.360	1.360	201	21.15	ZnO
	72.53	1.302	1.302	004	34.17	ZnO

	76.86	1.239	1.239	202	38.45	ZnO
ZnO-NPs 900°C	31.60	2.829	2.817	100	29.05	ZnO
	34.29	2.613	2.604	002	32.51	ZnO
	36.06	2.488	2.478	101	27.55	ZnO
	47.37	1.918	1.912	102	30.74	ZnO
	56.37	1.631	1.627	110	23.56	ZnO
	62.72	1.480	1.478	103	22.96	ZnO
	66.15	1.412	1.409	200	24.27	ZnO
	67.74	1.382	1.380	112	23.19	ZnO
	68.88	1.362	1.360	201	21.15	ZnO
	72.43	1.304	1.301	004	34.17	ZnO
	76.76	1.241	1.240	202	38.45	ZnO

The XRD data were used to calculate the crystalline and average crystallite sizes using the Scherrer equation (Asraf *et al*., 2015).

$$D = \frac{k\lambda}{\beta \cos\theta} \quad (1)$$

where;

D = crystalline size (nm)
k = Scherrer constant which is equal to 0.9
λ = wavelength of the x-ray which is equal to 0.15406 nm
β = full width at half maximum (FWHM) of the peak in radians
θ = peak position in radians

Electrochemical Performance of ZnO-NPs

The cycling stability of the prepared ZnO-NPs was further investigated by measuring their cycle performance up to 200th cycles. Figure 7 compares the cycling performance of ZnO-NPs calcined at 800°C and 900°C. The test cells were cycled at a 0.1 C rate between 0.01 and 3.00 V.

ZnO-NPs calcined at 800°C delivered a high initial charge/discharge capacity of 49/254 mAh g^{-1} while ZnO-NPs calcined at 900°C delivered a lower initial charge/discharge capacity of 52/205 mAh g^{-1}. For ZnO-NPs calcined at 800°C, the capacity drops quickly for the first 5 cycles and remained stable at approximately 48 mAh g^{-1} up to 200 cycles. The cyclability of ZnO-NPs calcined at 800°C is much better than ZnO-NPs calcined at 900°C; this could be due to the small particle sizes of ZnO will shorten the diffusion lengths of Na-ions and increases the active sites for the insertion/de-insertion of the ions (Durai *et al*., 2017).

Galvanostatic charge-discharge profiles for ZnO-NPs were shown in Figure 8 for selected charge-discharge cycles. The first discharge profiles differ from effective cycles and have a normal slope in the 0-3.0 V voltage range for both samples. The first cycle's degradation of the electrolyte and creation of a Solid Electrolyte Interface (SEI) on electrode particles can produce significant irreversible capacity (Qin *et al*., 2016). Compared to ZnO-NPs calcined at 900°C, the initial charge/discharge capacity of ZnO-NPs calcined at 800°C is higher and shows long plateaus, while ZnO-NPs calcined at 900°C exhibit shorter plateaus. The possible sodiation/desodiation mechanism of ZnO is described as follows (Qin *et al*., 2016).

$$ZnO + 2\ Na^+ + 2e^- \leftrightarrow Na_2O + Zn \quad (2)$$

$$Zn + Na^+ + e^- \leftrightarrow NaZn \quad (3)$$

Conclusion

In conclusion, ZnO-NPs using *Chromolaena odorata* leaves extract were obtained at calcination temperatures of 800°C and 900°C using a green synthesis approach. A dark brown precipitate formed at 80°C after heating in the oven and a white colour of ZnO-NPs powder

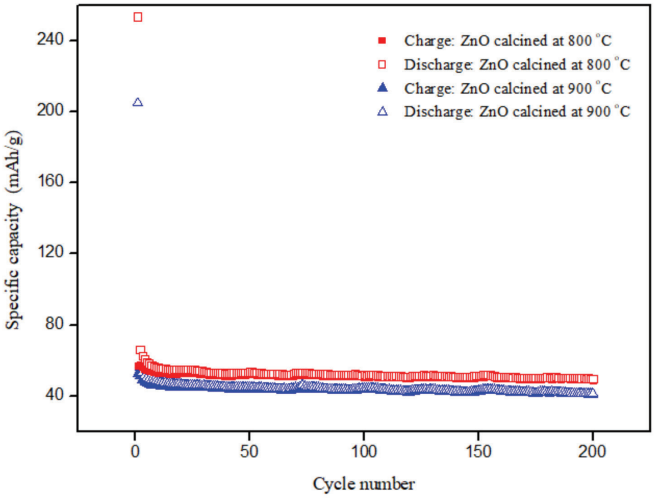

Figure 7: Cycling performances of ZnO-NPs calcined at 800°C and 900°C

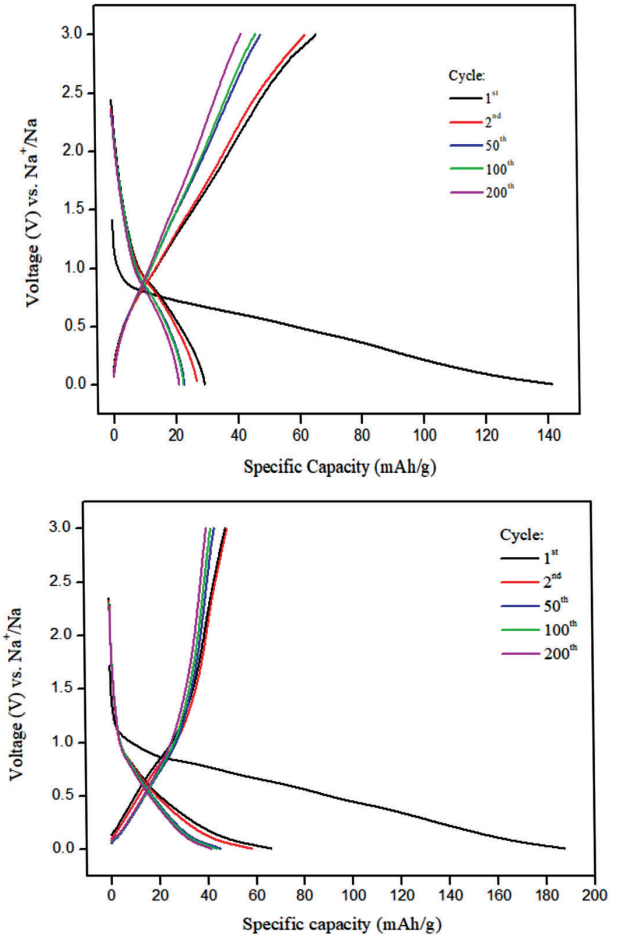

Figure 8: Galvanostatic charge-discharge profiles at (a) ZnO-NPs calcined at 800°C and (b) ZnO-NPs calcined at 900°C

was obtained after calcination. The influence of the temperature of the calcination on the ZnO-NPs was investigated. Analysis of FTIR spectroscopy showed ZnO stretching between 400 and 500 cm^{-1}. The XRD spectrum showed that the synthesised ZnO is in a hexagonal wurtzite structure with high crystallinity and a sharp peak of ZnO at (101), indicating the high crystallinity. TGA analysis revealed no significant weight loss observed for these samples after 550°C. SEM images showed different irregular shapes. In the cyclability study, the initial charge/discharge capacity of ZnO-NPs calcined at 800°C is higher and shows long plateaus, while ZnO-NPs calcined at 900°C exhibit shorter plateaus. These eco-friendly ZnO-NPs could be further exploited in size and shape as a future compatible candidate in SiBs.

Acknowledgements

The authors are thankful to the Universiti Malaysia Terengganu (UMT) Talent and Publication Enhancement Research Grants (TAPE-RG) Vot No. 55259 for financial support, the Faculty of Science and Marine Environment and the Faculty of Ocean Engineering Technology and Informatics for facilities provided in this project.

References

Agarwal, H., Kumar, S. V., & Rajeshkumar, S. (2017). A review on green synthesis of zinc oxide nanoparticles – An eco-friendly approach. *Resource-efficient Technologies, 3*(4), 406-413.

Ashraf, R., Riaz, S., Kayani, Z. N., & Naseem, S. (2015). Effect of calcination on properties of ZnO nanoparticles. *Materials Today: Proceedings*, *2*(10), 5468-5472.

Bandeira, M., Giovanela, M., Roesch-Ely, M., & Devine, D. M. (2020). Green synthesis of zinc oxide nanoparticles: A review of the synthesis methodology and mechanism of formation. *Sustainable Chemistry and Pharmacy*, *15*, 1-10.

Buniyamin, I., Akhir, R. M., Asli, N. A., Khusaimi, Z., & Rusop, M. (2022). Green synthesis of tin oxide nanoparticles by using leaves extract of *Chromolaena Odorata*: The effect of different thermal calcination temperature to the energy band gap. *Materials Today: Proceedings*, *48*, 1805-1809.

Chieng, B. W., & Loo, Y. Y. (2012). Synthesis of ZnO nanoparticles by modified polyol method. *Materials Letters*, *73*, 78-82.

Darvishi, E., Kahrizi, D., & Arkan, E. (2019). Comparison of different properties of zinc oxide nanoparticles synthesized by the green (using *Juglans regia* L. leaf extract) and chemical methods. *Journal of Molecular Liquids*, *286*, 110831.

Datta, A., Patra, C., Bharadwaj, H., Kaur, S., Dimri, N., & Khajuria, R. (2017). Green synthesis of zinc oxide nanoparticles using *Parthenium Hysterophorus* leaf extract and evaluation of their antibacterial properties. *Journal of Biotechnology & Biomaterials*, *7*(3), 271.

Dhanemozhi, A. C., Rajeswari, V., & Sathyajothi, S. (2017). Green synthesis of zinc oxide nanoparticle using green tea leaf extract for supercapacitor application. *Materials Today: Proceedings*, *4*(2), 660-667.

Dharmalingam, P., Palani, G., Apsari, R., Kannan, K., Lakkaboyana, S. K., Venkateswarlu, K., Kumar, V., & Ali, Y. (2022). Synthesis of metal oxides/ sulfides-based nanocomposites and their environmental applications: A review. *Materials Today Sustainability*, *20*, 100232.

Droepenu, E. K., Asare, E. A., Dampare, S. B., Adotey, D. K., Gyampoh, A. O., & Kumi-Arhin, E. (2021). Laboratory and commercial synthesized zinc oxide nanoparticles adsorption onto coconut husk: Characterization, isotherm, kinetic and thermodynamic studies. *Biointerface Research in Applied Chemistry*, *11*(1), 7871-7889.

Durai, B. L., Moorthy, B., Thomas, C. I., Kim, D. K., & Bharathi, K. K. (2017). Electrochemical properties of $BiFeO_3$ nanoparticles: Anode material for sodium-ion battery application. *Materials Science in Semiconductor Processing*, *68*, 165-171.

Fakhari, S., Jamzad, M., & Fard, H. K. (2019). Green synthesis of zinc oxide nanoparticles: A comparison. *Green Chemistry Letters and Reviews, 12*(1), 19-24.

Ganasan, E., Yusoff, H. M., Azmi, A. A., Chia, P. W., Lam, S. S., Kan, S.-Y., Liew, R. K., Venkateswarlu, K., & Teo, C. K. (2023). Food additives for the synthesis of metal nanoparticles: A review. *Environmental Chemistry Letters*, *21*(1), 525-538.

Gilavand, F., Saki, R., Mirzaei, S. Z., Lashgarian, H. E., Karkhane, M., & Marzban, A. (2021). Green synthesis of zinc nanoparticles using aqueous extract of *Magnolia officinalis* and assessment of its bioactivity potentials. *Biointerface Research in Applied Chemistry*, *11*(1), 7765-7774.

Kayani, Z. N., Saleemi, F., & Batool, I. (2015). Synthesis and characterization of ZnO nanoparticles. *Materials Today: Proceedings*, *2*(10), 5619-5621.

Nasrollahzadeh, M., Sajjadi, M., Sajadi, S. M., & Issaabadi, Z. (2019). Green nanotechnology. *Interface Science and Technology, 28*, 145-198. Elsevier.

Nava, O. J., Soto-Robles, C. A., Gómez-Gutiérrez, C. M., Vilchis-Nestor, A. R., Castro-Beltrán, A., Olivas, A., & Luque, P. A. (2017). Fruit peel extract mediated green synthesis of zinc oxide nanoparticles. *Journal of Molecular Structure*, *1147*, 1-6.

Qin, W., Li, D., Zhang, X., Yan, D., Hu, B., & Pan, L. (2016). ZnS nanoparticles embedded in reduced graphene oxide as high-performance anode material of sodium-ion Batteries. *Electrochimica Acta*, *191*, 435-443.

Ramanarayanan, R., Bhabhina, N. M., Dharsana, M. V., Nivedita, C. V., & Sindhu, S. (2018). Green synthesis of zinc oxide nanoparticles using extract of *Averrhoa bilimbi* (L) and their photoelectrode applications. *Materials Today: Proceedings*, *5*(8), 16472-16477.

Ramesh Naidu, B., & Venkateswarlu, K. (2022). WEPA: A reusable waste biomass-derived catalyst for external oxidant/metal-free quinoxaline synthesis via tandem condensation–cyclization–oxidation of α-hydroxy ketones. Quinoxaline characterization data, copies of 1H and 13C NMR spectra of quinoxalines, and XPS and XRF data. *Green Chemistry, 24*(16), 6215-6223.

Raut, S., Thorat, P. V., & Thakre, R. (2013). Green synthesis of zinc oxide (ZnO) nanoparticles using *Ocimum Tenuiflorum* leaves. *International Journal of Science and Research*, *4*(5), 2319-7064.

Rodrigues, A. G., Ruiz, R. C., Selari, P. J. R. G., De Araujo, W. L., & De Souza, A. O. (2021). Anti-biofilm action of biological silver nanoparticles produced by *Aspergillus tubingensis* and Antimicrobial Activity of Fabrics Carrying it. *Biointerface Research in Applied Chemistry*, *11*(6), 14764-14774.

Saidi, N. S. M., Yusoff, H. M., Bhat, I. U. H., Appalasamy, S., Mohamed Hassim, A. D., Yusoff, F., Asari, A., & Abdul Wahab, N. H. (2020). Stability and antibacterial properties of green synthesis silver nanoparticles using *Nephelium lappaceum* peel extract. *Malaysian Journal of Analytical Sciences, 24*(6), 940-953.

Sharma, U. R., & Sharma, N. (2021). Green synthesis, anti-cancer and corrosion inhibition activity of Cr_2O_3 nanoparticles. *Biointerface Research in Applied Chemistry*, *11*(1), 8402-8412.

Thirumavalavan, M., Huang, K. L., & Lee, J. F. (2013). Preparation and morphology studies of nano zinc oxide obtained using native and modified chitosan. *Materials*, *6*(9), 4198-4212.

Thiyagarajulu, N., Arumugam, S., Narayanan, A. L., Mathivanan, T., & Renuka R. R. (2021). Green synthesis of reduced graphene nanosheets using leaf extract of *Tridax procumbens* and its potential in vitro biological activities. *Biointerface Research in Applied Chemistry*, *11*(3), 9975-9984.

Vallinayagam, S., Rajendran, K., Lakkaboyana, S. K., Soontarapa, K., R. R, R., Sharma, V. K., Kumar, V., Venkateswarlu, K., & Koduru, J. R. (2021). Recent developments in magnetic nanoparticles and nano-composites for wastewater treatment. *Journal of Environmental Chemical Engineering*, *9*(6), 106553.

Vaseem, M., Umar, A., & Hahn, Y. B. (2010). ZnO nanoparticles: growth, properties, and applications. *Metal Oxide Nanostructures and Their Applications*, *5*(1).

Wang, L., Wei, Z., Mao, M., Wang, H., Li, Y., & Ma, J. (2019). Metal oxide/graphene composite anode materials for sodium-ion batteries. *Energy Storage Materials, 16*, 434-454.

Wang, L., Yang, C., Dou, S., Wang, S., Zhang, J., Gao, X., Ma, J., & Yu, Y. (2016). Nitrogen-doped hierarchically porous carbon networks: synthesis and applications in lithium-ion battery, sodium-ion battery and zinc-air battery. *Electrochemical Acta*, *219*, 592-603.

Yedurkar, M. S., Punjabi, D. K., Maurya, B. C., & Mahanwar, A. P. (2018). Biosynthesis of zinc oxide nanoparticles using *Euphorbia Milii* Leaf Extract - A green approach. *Materials Today: Proceedings, 5*(10), 22561-22569.

Yusoff, F., Rosli, A. R., & Ghadimi, H. (2021). Synthesis and characterisation of gold nanoparticles/poly3,4-ethylene-dioxythiophene/reduced-graphene oxide for electrochemical detection of dopamine. *Journal of the Electrochemical Society, 168*(2), 026509.

Yusoff, H. M., Chandran, P. D. B., Sayuti, F. A., Kan, S-U., Radzi, S. A. M., Yong, F-S. J., Lee, O. J., & Chia, P. W. (2021). A highly efficient, recyclable and alternative method of synthesizing phenols from phenylboronic acids using non-endangered metal: Samarium oxide. *Inorganic Chemistry Communications*, *130*, 108749.

Yusoff, H. M., Idris, N. H., Hipul, N. F., Mahamad Yusoff, N. F., Mohd. Izham, N. Z., & Bhat, I. U. H. (2020). Green synthesis of zinc oxide nanoparticles using black tea extract and its potential as anode material in sodium-ion batteries. *Malaysia Journal of Chemistry*, *22*(2), 43-51.

Yusoff, H. M., Rafit, F. A., Mohamad, F. I., Hassan, N., & Daud, A. I. (2015). The effect of calcination temperatures in the synthesis of nanocrystalline magnesium oxide via sol-gel technique. *Applied Mechanics and Materials*, *865*, 36-42.